

Forecasting Actions and Characteristic 3D Poses

Christian Diller
Technical University of Munich
christian.diller@tum.de

Thomas Funkhouser
Google
tfunkhouser@google.com

Angela Dai
Technical University of Munich
angela.dai@tum.de

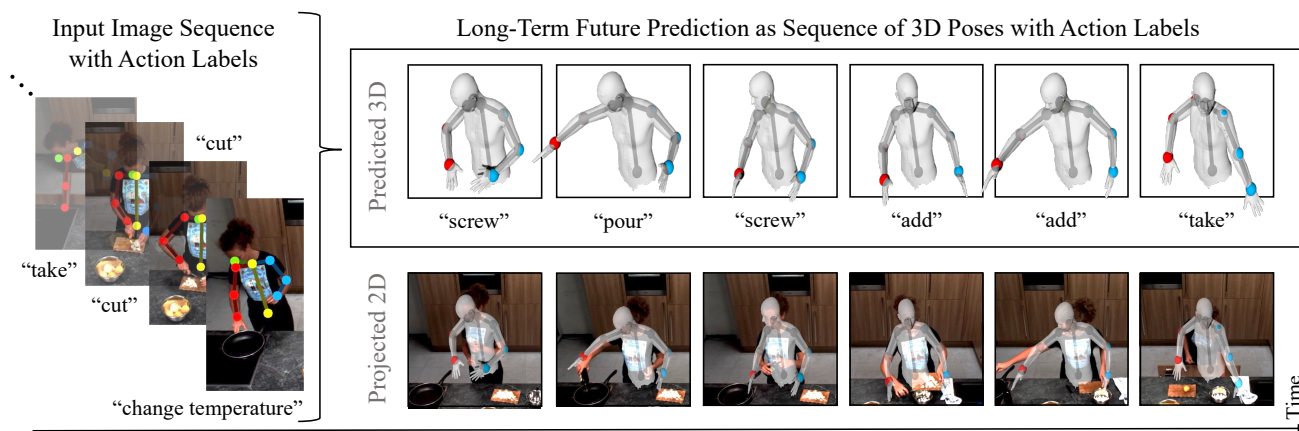


Figure 1. We propose to model long-term future human behavior by jointly predicting a sequence of future action labels and their realization as the 3D poses that characterize these actions (characteristic 3D poses). From an input RGB sequence and corresponding actions, we detect 2D poses that are lifted into future 3D pose predictions in forecasted future behavior.

Abstract

We propose to model longer-term future human behavior by jointly predicting action labels and 3D characteristic poses (3D poses representative of the associated actions). While previous work has considered action and 3D pose forecasting separately, we observe that the nature of the two tasks is coupled, and thus we predict them together. Starting from an input 2D video observation, we jointly predict a future sequence of actions along with 3D poses characterizing these actions. Since coupled action labels and 3D pose annotations are difficult and expensive to acquire for videos of complex action sequences, we train our approach with action labels and 2D pose supervision from two existing action video datasets, in tandem with an adversarial loss that encourages likely 3D predicted poses. Our experiments demonstrate the complementary nature of joint action and characteristic 3D pose prediction: our joint approach outperforms each task treated individually, enables robust longer-term sequence prediction, and outperforms alternative approaches to forecast actions and characteristic 3D poses.

1. Introduction

Predicting future human behavior is fundamental to machine intelligence, with many applications in autonomous driving, robotics, mixed reality, and more. For instance, an autonomous vehicle must predict whether or not a pedestrian will cross the street based on previous observations, or a robotic assistant should predict future human behavior while they perform an activity such as cooking, in order to assist with ingredients or tools at the right time. This requires not only predicting the action(s) that will be taken, but also estimating the corresponding human poses that will occur in realizing such actions, at least several seconds prior to the future behavior to enable potential anticipatory action.

We thus propose to jointly forecast action labels along with the 3D poses characterizing these longer-term future actions, from an input RGB sequence observation. Prior work has focused on each task separately: activity forecasting predicts future action labels without considering the 3D poses realizing these actions [16, 17, 24, 25, 35], while 3D pose forecasting focuses on fixed frame rate sequence prediction limited to single actions in short-term time frames without considering longer-term action sequences [14, 29, 31, 46].

We observe that the nature of these two tasks are coupled: predicting action labels with realized 3D poses helps to encourage richer feature learning and can materialize sub-category level differences in actions for predicting future activities, and grounding 3D poses with actions provides global structure for longer-term forecasting. As shown in Fig. 1, from a sequence of RGB image observations and their actions, our method jointly predicts a future sequence of action labels and their realization as *characteristic 3D poses* [11], which are a characteristic representation of the action being performed (i.e., rather than an arbitrary pose while performing an action, one in which the action is distinctly recognizable or articulated). This form of 3D action pose representation allows for an efficient modelling of long-term action sequences by focusing on moments of interest. Together with joint action label prediction, this leads to a more global view on composite action sequences, rather than just predicting plausible human body motion.

To learn the mapping from past RGB images to future 3D poses and action labels, it would be ideal to have a training dataset with ground truth 3D pose and action annotations for complex sequences of actions observed in RGB videos. Unfortunately, no such dataset exists, to the best of our knowledge. There are RGB video datasets with tracked 3D poses for limited types of actions (e.g., walking or waving); and there are video datasets with action labels for complex sequences of actions (e.g., cooking). However, there is no single dataset that has both types of annotations, and capturing one would be difficult due to the challenges of setting up 3D pose trackers in settings where people typically perform complex sequences of actions (e.g., cooking in a kitchen). Instead, we must learn to lift 2D video observations to 3D poses and action labels without paired data. To do so, we train our network on two RGB video datasets mainly used for action recognition (MPII Cooking 2 [36] and IKEA-ASM [7]) using losses that measure: 1) how well future actions are predicted, 2) how well 2D projections of 3D characteristic pose predictions match 2D future video frames, and 3) how likely those 3D characteristic pose predictions are with respect to a distribution learned from separate 3D pose tracking datasets (Human3.6m [20], AMASS [28], and GRAB [38]). This approach does not require any correspondence between the 2D video and 3D pose data.

Our experiments demonstrate that joint learning of action behavior and 3D poses with this approach is complementary – our proposed method outperforms state-of-the-art methods applied to each task separately. Additionally, we find predicting actions and their characteristic poses enables more robust autoregressive prediction for longer-term forecasting. In summary, our contributions are:

- We propose to forecast future human behavior by jointly predicting a sequence of action labels and the characteristic 3D poses that represent the actions.

- We do not require any paired 3D poses to 2D action videos to learn this joint forecasting, instead leveraging differentiable 2D projection coupled with adversarial regularization to predict plausible 3D future human behavior.
- We demonstrate that jointly action labels and characteristic 3D poses results in effective complementary feature learning, outperforming each task treated individually and producing robust longer-term sequence prediction.

2. Related Work

3D Human Pose Forecasting. Forecasting 3D human poses has been studied in many previous works that not only recognize observed 3D poses but also predict future ones. The pose forecasting task is often formulated as a 3D sequential motion prediction task, taking an input 3D sequence of poses and predicting an output 3D sequence of poses at a fixed frame rate, e.g., that of a camera capture. For short-term future prediction (up to ≈ 1 second), recurrent neural network-based approaches have achieved impressive performance [2, 10, 15, 18, 22, 32, 43]. As RNNs tend to struggle to capture longer-term dependencies with a fixed size history, graph and attention-based approaches have been proposed to encode temporal history [29, 31, 39]. Additionally, various approaches have been proposed to model future human motion stochastically to produce diverse future sequence predictions [3, 6, 30, 45, 46].

These approaches tend to follow a time-based paradigm, which can make longer-term prediction difficult – for instance, a series of several actions may be performed under a variety of plausible speeds, which induces a significant ambiguity in a time-based prediction. To address this issue, [11] introduced the task of forecasting characteristic 3D poses, which are salient keyframe poses corresponding to the next actions to be performed. These goal-based poses are more semantically meaningful and consistent across different action sequences than time-based ones, and thus are better for long-term forecasting [11]. However, they focus only on predicting 3D human poses from 3D observed inputs, and train with 3D pose supervision, which limits applicability to common scenarios where 3D inputs and ground-truth are not available. In contrast, we aim to forecast from 2D observed inputs only. Additionally, we make use of an autoregressive forecasting approach to enable longer-term sequence prediction of such characteristic 3D poses.

Human Action Forecasting. Action forecasting has been studied by many approaches to predict future actions from an input video sequence. Various methods have developed to learn effective representations, including Hidden Markov Models [25], recurrent neural networks [1, 21, 44],

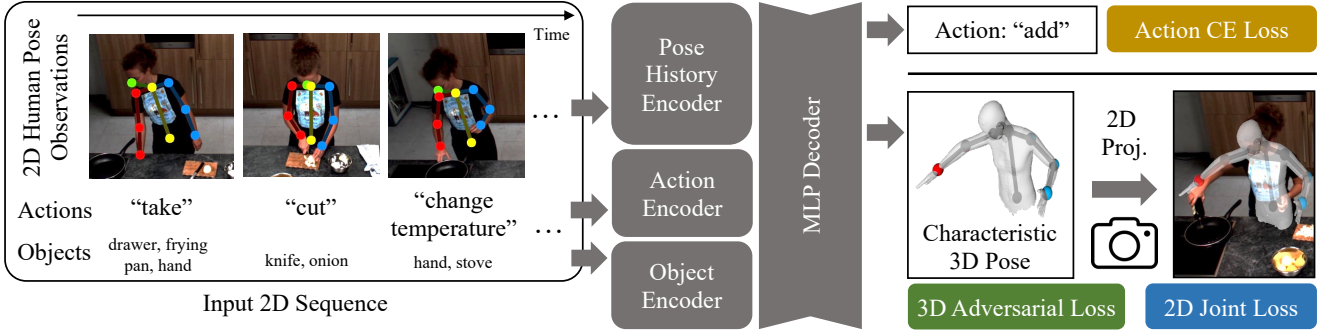


Figure 2. Our approach takes as input a sequence of RGB images, from which 2D poses are extracted, as well as their corresponding action label and objects. Each input is encoded and fused together to jointly predict the next action label and characteristic 3D pose. 2D action video data is used to supervise the action and pose such that its projection matches the ground truth future frame, with an adversarial 3D loss encouraging valid 3D pose prediction.

transformer-based networks [17], and self-supervised feature learning [19, 40]. Such method focus only on characterizing anticipation with action labels only, while we aim to predict a richer characterization of the anticipated future in incorporating a characteristic 3D pose representative of a future action goal in a sequence of action-pose predictions.

Joint Action and 2D Human Pose Forecasting. The advantages of jointly forecasting human actions with their 2D pose realizations has been studied in several works [26, 47]. Zhu et al. [47] proposed a method for forecasting 2D human poses together with corresponding action labels, for actions up to 1 second in the future. In [26], the authors show the usefulness of jointly predicting 2D hand placement and actions. Our goal is to predict a 3D representation of the characteristic pose associated with the predicted action for longer-term forecasting of multiple action steps, many seconds into the future. We demonstrate the complementary nature of 3D reasoning, which also enables a wide variety of potential applications by providing spatial information, which is lacking in the 2D representation.

Goal-Driven Future Prediction. Goal-driven forecasting has also been explored beyond action label forecasting. In addition to the previously-mentioned characteristic 3D pose prediction of [11], goal-oriented forecasting has been leveraged to predict goal locations for future human walking trajectories [8], as well as future video sequences by predicting goal events as keyframes [5, 13, 23, 34]. We build upon these ideas by introducing a new goal-driven method for joint action anticipation and characteristic 3D pose forecasting.

Our approach is the first to address 3D pose forecasting without 3D input observations - a notably more challenging task than pose estimation from an image, as future motion that does not match the 2D observations must be generated. We demonstrate that simultaneously predicting 3D poses and actions is complementary and believe this will facilitate further research in 3D pose forecasting.

3. Method Overview

Our method aims to learn to jointly model future human actions along with the characteristic 3D poses representative of those actions. From a sequence of RGB image observations of a person performing a series of actions and the corresponding action labels, we predict a sequence of future action labels and 3D poses characteristic of these actions. This enables joint reasoning of not only global semantic behavior but also the physical manifestation of forecasted behavior.

An overview of our approach is shown in Fig. 2. For an input sequence $S = \{(I_i, a_i, o_i)\}$ of N RGB images I_i with the corresponding actions a_i and involved objects o_i , we aim to predict the future M actions $\{\hat{a}_k\}$ that will be taken along with their characteristic poses in 3D $\{\hat{Y}_k\}$. We define the human pose as a collection of J body joints at salient locations, so each output pose \hat{Y}_k is predicted as a set of J 3D coordinates.

From the input images, we extract information about the previous 2D pose movement by detecting 2D poses $\{X_i\}$, each with J 2D joints, with the state-of-the-art 2D pose estimator OpenPose [9]. We then encode this information along with previously observed action and object labels to predict the next future action label \hat{a}_k and characteristic 3D pose \hat{Y}_k . We can then forecast a future sequence by autoregressively predicting a series, considering the 2D projections of the previously predicted 3D poses along with previously predicted actions as input to a new prediction.

In the absence of coupled 3D pose data to complex 2D action video, we supervise forecasted poses to align to the detected 2D poses in future video, and constrain the poses to be valid in 3D with an adversarial loss against an arbitrary set of 3D poses. This does not require any correspondence between 3D pose data and 2D video, and we can thus train with a database of unrelated 3D poses.

4. Joint Forecasting of Actions and Characteristic 3D Poses

Our network takes as input the previous 2D observations $\{X_i\}$ extracted from the $\{I_i\}$ images, as well as action and object labels $\{a_i\}$ and $\{o_i\}$. Since we only predict action labels, object labels are given from the objects seen at the beginning of the sequence, and subsequently re-used for the entire sequence. Each of these are encoded in parallel with three separate encoders; the actions and objects with simple MLPs while the poses are projected into latent space with a single linear layer and then processed with a stack of three residual blocks. These encoded features are then all concatenated together, and processed jointly with an MLP to produce a latent code z . Finally, we decode both poses and actions in parallel based on z using an MLP decoder each, yielding the next action label class as a vector $\hat{a}_k \in \mathbb{R}^{N_a}$ and 3D characteristic pose $\hat{Y}_k \in \mathbb{R}^{J \times 3}$, with N_a the number of action classes. For a more detailed architecture specification, we refer to the appendix.

We jointly learn future action labels and characteristic 3D poses by supervising \hat{a}_k and \hat{Y}_k to match the observed future 2D video, and constrain \hat{Y}_k to form a valid 3D pose by an adversarial loss, optimizing for the overall loss:

$$\mathcal{L} = \lambda_{action} \mathcal{L}_{action} + \lambda_{pose2d} \mathcal{L}_{pose2d} + \lambda_{adv3d} \mathcal{L}_{adv3d}, \quad (1)$$

where \mathcal{L}_{action} denotes the action loss, as described in Sec. 4.1, \mathcal{L}_{pose2d} and \mathcal{L}_{adv3d} constraining the predicted pose, as described in Sec. 4.2, and the λ weighting each loss.

4.1. Action Forecasting

Predicted future actions are decoded from the latent code z by an MLP decoder to predict the action class \hat{a}_k , supervised by cross entropy with the ground truth future action: $\mathcal{L}_{action} = \text{CE}(\hat{a}_k, a_k^{\text{gt}})$.

4.2. Characteristic Pose Forecasting

Our goal is to forecast complex action behavior not only in terms of action labels, but also manifested as a sequence of characteristic poses in 3D. Since we only have 2D pose annotations available, we first constrain these poses to represent future actions in 2D and make use of an adversarial regularization in 3D. This does not require any correspondence between 2D and 3D data, only a collection of valid 3D poses, which are readily available.

Differentiable 2D Projection

Our generator network predicts the next characteristic action pose \hat{Y}_k as a set of 3D joints. To constrain \hat{Y}_k based on the target future 2D pose X^{gt} extracted from the ground truth future image, we differentially project \hat{Y}_k into the 2D

image with given camera parameter intrinsic K and extrinsic rotation and translation R, t :

$$\hat{X} = K(R\hat{Y}_k + t) \quad (2)$$

Since we learn from third-person video with a fixed camera, we can use the same camera parameters for all sequences used for training. We can then define the 2D pose loss as the mean squared error between the projected pose prediction and the ground truth:

$$\mathcal{L}_{pose2d} = \|X^{\text{gt}} - \hat{X}_k\|_2^2 \quad (3)$$

Note that we only predict the J joints that have been observed in the video data (excluding any joints that remain occluded in the observed video data), so this loss can be applied to all predicted joints.

Adversarial 3D Pose Regularization

While the action and pose prediction loss provide effective predictions when considered in the 2D projections, the \hat{Y}_k remain underconstrained in 3D and thus tend to exhibit large distortions and implausible bone lengths and angles, when trained with only 2D supervision. We thus constrain the predicted poses to form valid 3D poses by formulating an adversarial 3D loss from a critic network which that is simultaneously trained to distinguish predicted poses from a database of real 3D skeleton samples. Note that there is no correspondence between these skeletons and the 2D poses extracted from the action video sequences – any database of 3D skeletons can be used. We can thus train our approach with an entirely uncorrelated 3D pose dataset without requiring 3D pose annotation to action video.

We then formulate \mathcal{L}_{adv3d} as a Wasserstein loss [4], training the critic network in an alternating fashion with the generator. This enables effective forecasting of future 3D characteristic poses for predicted future action labels, without requiring any 3D observations as input.

In order to enable the critic network to learn effectively about likely intrinsic pose constraints (e.g., lengths, kinematic chains, or valid joint angles), the critic takes as input not only the 3D joint locations of \hat{Y}_k but also their kinematic statistics as a matrix Ψ , following [41, 42].

Ψ encodes joint angles and bone lengths as $\Psi = B^T B$, where $B = (b_1, b_2, \dots, b_b)$ is a matrix with columns $b_i = j_k - j_l$ representing the vectors between each joint j_k and j_l . Ψ then contains bone lengths l_i^2 on its diagonal, and angular representations on the off-diagonal entries.

4.3. Sequence Prediction

In order to forecast longer-term future behavior, our 3D pose predictions enable a natural autoregressive sequence prediction by taking the predictions \hat{X}_t, \hat{a}_t at time step t as

	MPII Cooking II				IKEA ASM			
	2d	3d	Action Accuracy		2d	3d	Action Accuracy	
Approach	MPJPE [px] ↓	Quality ↑	top-1 ↑	top-5 ↑	MPJPE [px] ↓	Quality ↑	top-1 ↑	top-5 ↑
Zero Velocity	118	–	–	–	74	–	–	–
Train Average	166	–	–	–	91	–	–	–
AVT [17] RGB	–	–	19%	48%	–	–	22%	60%
AVT [17] RGB+Skeleton	–	–	20%	46%	–	–	23%	59%
RepNet [42] + DLow [46]	89	0.70	–	–	51	0.30	–	–
RepNet [42] + GSPS [30]	75	0.57	–	–	55	0.11	–	–
Ours	50	0.55	29%	62%	40	0.31	29%	63%

Table 1. Quantitative comparison with state-of-the-art action anticipation and 3D pose forecasting methods. Our joint forecasting approach enables more accurate future action and pose predictions.

part of the input for time step $t + 1$. We can thus predict a sequence of M future action labels and characteristic 3D poses; we use $M = 10$ for MPII Cooking II [36] and $M = 5$ for IKEA-ASM [7], respectively.

4.4. Training Details

We train our approach for the $J = 9$ joints commonly seen across the input observed video data, characterizing the upper body in MPII Cooking II [36] and IKEA-ASM [7].

Additionally, we use loss weights $\lambda_{action} = 1e^6$, $\lambda_{pose} = 1$, and $\lambda_{adv3d} = 1$, empirically chosen to numerically balance each individual loss with the others.

We train our approach on a single NVIDIA GeForce RTX 2080TI for ≈ 12 hours until convergence. We use an ADAM optimizer with batch size 4096, weight decay 0.001, and a constant learning rate of 0.0001 for both generator and discriminator.

4.5. Data Preprocessing

We train and evaluate our approach on two datasets: MPII Cooking II [36] and IKEA-ASM [7]. Both datasets contain sequences of human actors performing complex actions, and provide annotations of finer-grained sub-actions. More specifically, MPII Cooking II [36] is an action recognition dataset with 272 complex cooking sequences, where each sequence contains an average of 35 annotated sub-actions. In each sequence, one global cooking action is performed by one human actor; action sequences are not scripted, leading to diverse and natural human behavior. IKEA-ASM contains 370 unscripted sequences of actors assembling IKEA furniture, with an average of 15 annotated sub-actions.

In both datasets, each action sequence has been filmed from a fixed camera setup; the third-person point of view enables straightforward extraction of 2D poses with an off-the-shelf 2D pose estimator, in our case OpenPose [9].

We consider the 9 upper-body joints of the OpenPose skeletons, as the other joints are almost always occluded in the video observations, and remove global translation by centering each 2D pose at the neck joint.

Characteristic poses, in contrast to an arbitrary pose within a labeled action range, should be the most representative pose of that action, and are annotated for each sub-action in each sequence as the most articulated pose representing the action. All annotations were performed by the authors within a time span of 5 days, yielding a total of $\approx 18,000$ characteristic poses ($\approx 12,000$ from MPII Cooking II and $\approx 6,000$ from IKEA-ASM) across all action sequences.

For the 3D adversarial loss, we used a set of $\approx 800,000$ human poses from popular 3D pose datasets: Human3.6m [20], AMASS [28], and GRAB [38]. Note that none of these 3D poses have any correspondence with the 2D posed actions from the MPII Cooking II dataset, instead depicting various human skeletons in natural and diverse poses.

5. Results

We evaluate sequence forecasting of action labels and characteristic 3D poses on the MPII Cooking II [36] dataset, which contains action annotations for complex third-person video of people cooking. To evaluate predicted 3D pose quality, we compare to ground truth high-fidelity, motion-tracked poses from GRAB [38] to represent real pose quality.

5.1. Evaluation Metrics

2D Pose Error. We evaluate predicted pose error projected into 2D, in comparison with 2D poses extracted from ground truth future frames using [9]. We use the mean per-joint position error (MPJPE) [20] in 2D: $EM_{PJPE} = \frac{1}{M} \sum_{j=1}^M \|\hat{X} - X^{gt}\|_2^2$.

3D Pose Quality. In the absence of annotated ground truth 3D poses for the action video sequences, we measure the quality of predicted 3D poses as how distinguishable they are in comparison to a set of real 3D poses. We follow [3] and evaluate quality by training a binary classifier on 50,000 human poses generated at different training steps (representing examples of unrealistic 3D poses) and 50,000 real 3D pose samples. For classification accuracy a of this classifier, quality is measured as $1 - a$, with a quality of 1 indicating full indistinguishability from real poses.

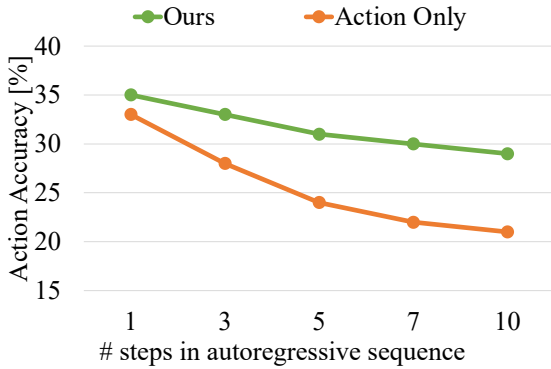


Figure 3. Action accuracy over time. Our joint action-characteristic pose forecasting enables more robust autoregressive action forecasting than action prediction without considering pose.

Action Accuracy. We report the action accuracy of the predicted sequences, as the mean over all sequences in the test set. We evaluate the top- n accuracy based on whether the ground truth action is among the n highest scoring predictions, for $n = 1$ and $n = 5$, following [17].

5.2. Comparison to State-of-the-Art 3D Pose Forecasting

Tab. 1 compares our method to state-of-the-art 3D pose forecasting methods DLow [46] and GSPS [30]. Since both methods expect sequences of observed 3D human poses as input, we first apply a state-of-the-art 3D pose estimator [42] on our extracted 2D input poses, producing 3D pose inputs and supervision for training these forecasting methods.

We then train both 3D pose prediction methods from scratch on this generated data, using their original parameter settings. Each method takes as input a pose history of M poses and outputs a sequence of M poses, analogous to our setup where each pose is a characteristic pose corresponding to an action step ($M = 10$ for MPII Cooking II and $M = 5$ for IKEA-ASM). Our approach to lift 2D to future 3D poses and actions in an end-to-end fashion enables more effective pose forecasting than these state-of-the-art 3D pose

Poses	2D	3D	Action Accuracy	
	MPJPE [px] ↓	Quality ↑	top-1 ↑	top-5 ↑
Uncoupled	75	0.29	28%	59%
Middle	58	0.45	26%	57%
Random	67	0.37	22%	55%
Characteristic	50	0.55	29%	62%

Table 2. Ablation on pose forecasting on MPII Cooking II [36]. We consider pose prediction following state-of-the-art pose forecasting as decoupled from actions (uncoupled), as well as poses coupled to actions in various fashions: middle (the middle pose of an action range), random (a random pose of the action), and our characteristic pose prediction, which most benefits action prediction.

forecasting approaches on both datasets.

Statistical 2D Baselines. We additionally compare with two statistical baselines in 2D, following [11]: the average target train pose, and a zero-velocity baseline which was introduced by Martinez et al. [32] as competitive with state of the art. We outperform both baselines, indicating that our method learns a strong action pose representation.

5.3. Comparison to State-of-the-Art Action Label Forecasting

We compare the action accuracy of our joint action-pose forecasting to AVT [17], a state-of-the-art action anticipation method, in Tab. 1. We train and evaluate AVT on input RGB frames and their action and object labels, similar to our training setup, and use their original training settings initialized with a pre-trained vision transformer [12]. Additionally, as we consider extracted 2D poses from the input RGB images, we also evaluate a variant of AVT that is trained and evaluated on RGB images and 2D pose images (+Skeleton). Our approach outperforms AVT in both these scenarios, by jointly predicting future actions and characteristic 3D poses.

We followed the training and evaluation protocol of AVT, and report AVT scores using their autoregressive action label prediction method.

5.4. Ablation Studies

What is the effect of pose forecasting on long-term action understanding? Tab. 3 shows that there is a notable improvement in action accuracy between training only with an action loss vs. training action and 2D pose loss jointly. This becomes more apparent when training action only vs action and full pose prediction (2D and 3D losses). In addition, Fig. 3 shows the correspondence between autoregressive prediction length and action accuracy: jointly forecasting poses and actions is enables more robust autoregressive forecasting over time. We conclude that pose forecasting is beneficial for long-term action understanding.

How does action forecasting affect pose prediction performance? Tab. 3 demonstrates that pose forecasting trained jointly with action prediction is complementary and enables more accurate pose prediction.

What is the effect of characteristic pose forecasting? Since state-of-the-art pose forecasting focuses on fixed frame rate predictions independent of actions, we compare with such joint forecasting of action and pose where predicted poses are sampled at equally spaced points in time in Tab. 2 (uncoupled). Additionally, we consider alternative poses to forecast for each action rather than a characteristic 3D pose (middle of the action, random in the action). Forecasting characteristic 3D poses along with action labels enables the most benefit to action forecasting.

			MPII Cooking II				IKEA ASM			
Losses During Training			2D	3D	Action Accuracy		2D	3D	Action Accuracy	
Action	2D Proj.	3D Adv.	MPJPE [px] ↓	Quality ↑	top-1 ↑	top-5 ↑	MPJPE [px] ↓	Quality ↑	top-1 ↑	top-5 ↑
✓	×	×	–	–	21%	50%	–	–	24%	59%
✓	✓	×	62	0.10	26%	60%	46	0.05	27%	60%
×	✓	×	54	0.21	–	–	44	0.09	–	–
×	✓	✓	58	0.53	–	–	43	0.29	–	–
✓	✓	✓	50	0.55	29%	62%	40	0.31	29%	63%

Table 3. Ablation on the effect of the action, 2D projection, and 3D adversarial losses. Combining all together for joint forecasting enables complementary learning to produce the best performance.

5.5. Qualitative Results

Qualitative evaluations for the predicted poses are shown in Fig. 5 on data from MPII Cooking II [36] and in Fig. 4 on data from IKEA-ASM [7]. We compare our approach with state-of-the-art 3D pose forecasting of DLow [46] and GSPS [30]. For each method, we show a 3D body mesh in addition to the predicted 3D pose joints, to more comprehensively show the 3D structure of the forecasting results; we obtain the body meshes by fitting an SMPL [27] model to each methods’ predicted 3D body joints.

As there is no 3D ground truth available, we show the camera perspective with background for context as well as without background for a 3D pose only version. The two views demonstrate the fit to the ground truth 2D along with the quality of the 3D pose, respectively. Our approach

leads to poses that better follow the ground-truth action poses in 2D compared to both previous methods while still maintaining a valid pose structure in 3D. Notably, this is true for both datasets, as our approach effectively forecasts the different data characteristics of both cooking as well as furniture assembly. In particular, our joint action-3D pose forecasting enables more accurate forecasting with diverse and accurate 3D pose structures.

5.6. Limitations

While we have demonstrated the potential of joint action and 3D pose forecasting, several limitations remain. For instance, our method leverages a separate 2D pose extraction as input to training, while an end-to-end formulation could potentially better leverage other useful signal in the input frames. Additionally, a more holistic body representation

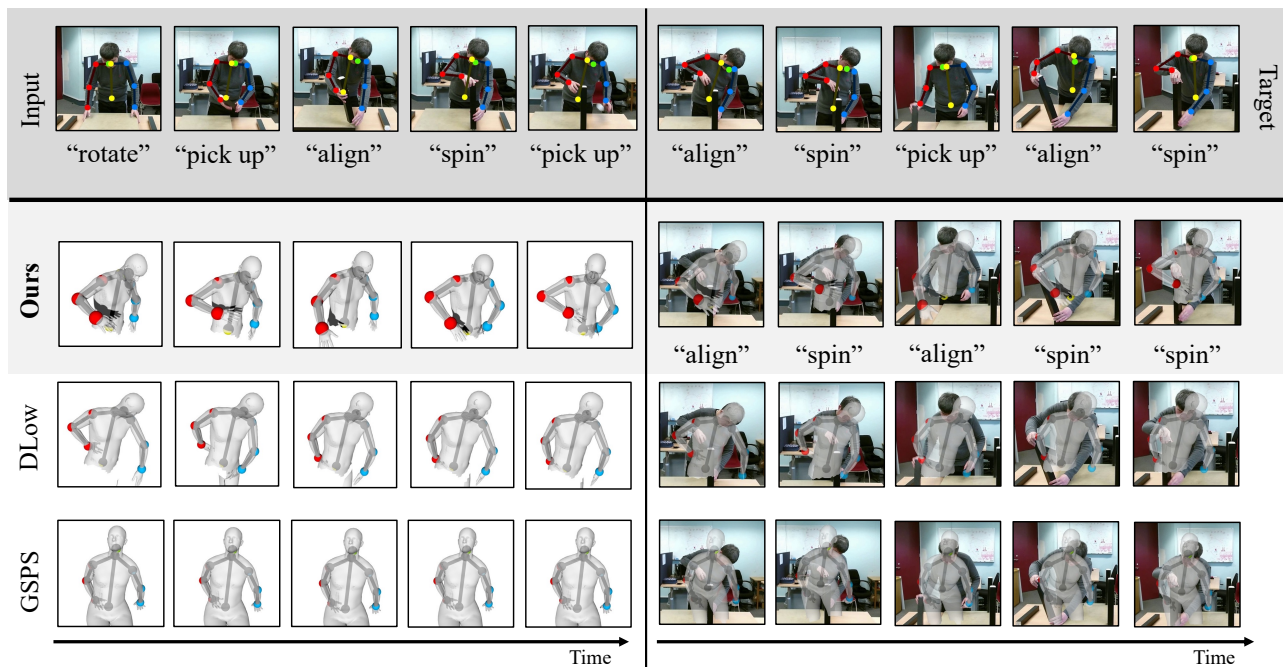


Figure 4. Qualitative comparison between DLow [46], GSPS [30], and our method on IKEA-ASM [7] data. For each method, we show the 3D predicted pose projected into the 2D target view, without background (left column) and with background for context (right column). Our joint reasoning captures the individual characteristic action poses more faithfully while producing spatially plausible 3D poses.

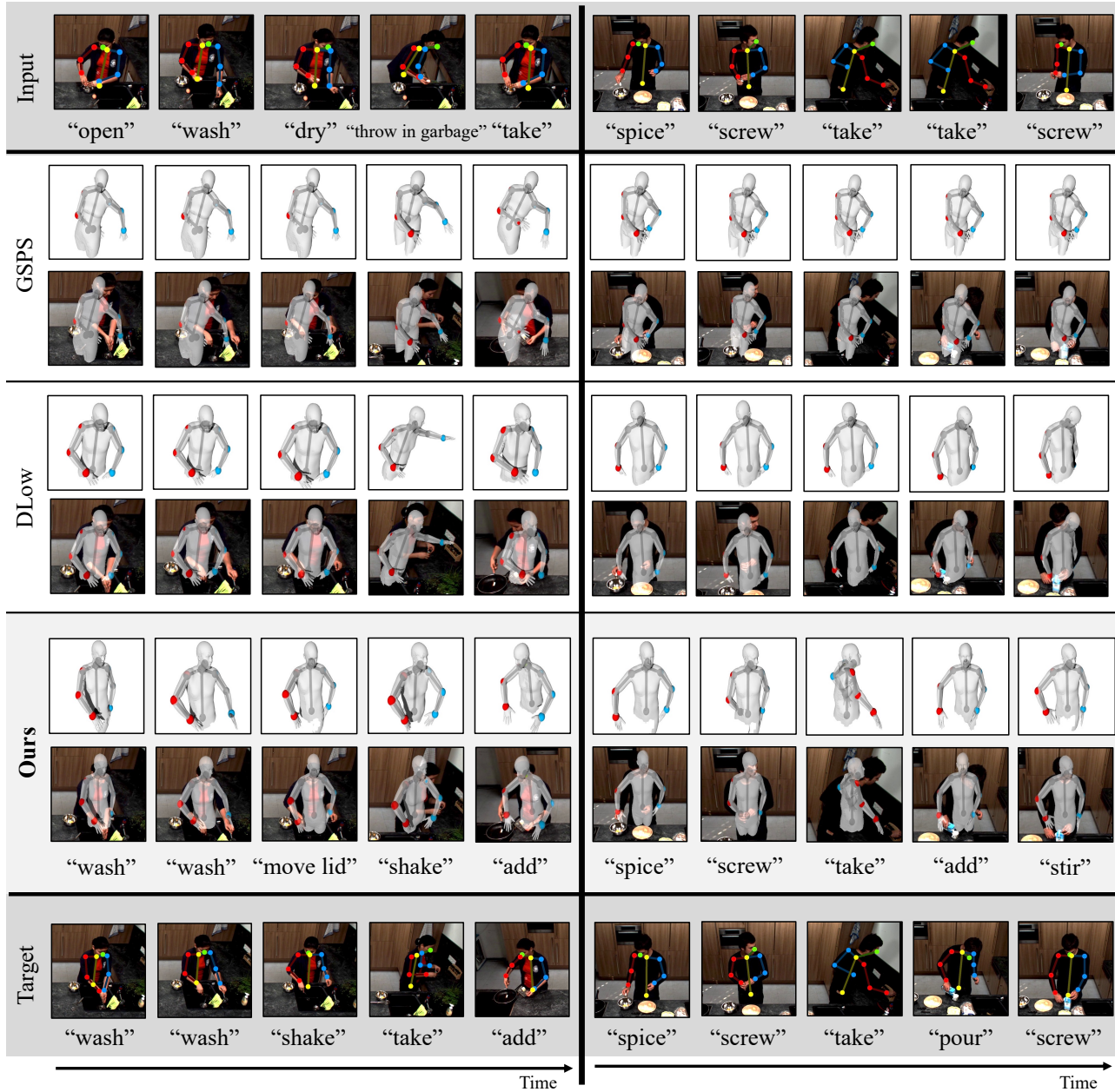


Figure 5. Qualitative comparison between DLow [46], GSPS [30], and our method on two sequences (left and right) from MPII Cooking II [36]. For each method, we show the 3D predicted pose projected into 2D, without background (first row) and with background for context (second row). By considering both 3D pose and action forecasting together, we more effectively forecast the longer-term behavior.

than pose joints would be important for finer-grained interactions that involve reasoning over small limbs (e.g., hands) and body surface contact.

6. Conclusion

In this paper, we proposed a new approach to forecast future human behavior by jointly predicting future action labels as well as characteristic 3D poses which physically represent the actions to be performed. Our action and 3D

pose forecasting does not require any 3D-annotated action video sequences, or 3D input data; instead, we learn complex action sequences from 2D action video data, and constrain predicted poses to be valid with an adversarial formulation against uncorrelated 3D pose data. Experiments demonstrate that jointly forecasting action labels and characteristic 3D poses enables complementary feature learning, outperforming each individual task considered separately, and producing more robust long-term forecasting.

Acknowledgements

This project is funded by the Bavarian State Ministry of Science and the Arts and coordinated by the Bavarian Research Institute for Digital Transformation (bidt), and the German Research Foundation (DFG) Grant Learning How to Interact with Scenes through Part-Based Understanding.

References

- [1] Yazan Abu Farha, Alexander Richard, and Juergen Gall. When will you do what?-anticipating temporal occurrences of activities. In *Proceedings of the IEEE conference on computer vision and pattern recognition*, pages 5343–5352, 2018. [2](#)
- [2] Emre Aksan, Manuel Kaufmann, and Otmar Hilliges. Structured prediction helps 3d human motion modelling. In *2019 IEEE/CVF International Conference on Computer Vision, ICCV 2019, Seoul, Korea (South), October 27 - November 2, 2019*, pages 7143–7152. IEEE, 2019. [2](#)
- [3] Sadegh Aliakbarian, Fatemeh Sadat Saleh, Mathieu Salzmann, Lars Petersson, and Stephen Gould. A stochastic conditioning scheme for diverse human motion prediction. In *Proceedings of the IEEE/CVF Conference on Computer Vision and Pattern Recognition*, pages 5223–5232, 2020. [2](#), [5](#)
- [4] Martin Arjovsky, Soumith Chintala, and Léon Bottou. Wasserstein generative adversarial networks. In *International conference on machine learning*, pages 214–223. PMLR, 2017. [4](#)
- [5] Amir Bar, Roi Herzig, Xiaolong Wang, Anna Rohrbach, Gal Chechik, Trevor Darrell, and Amir Globerson. Compositional video synthesis with action graphs. In *International conference on machine learning*, 2021. [3](#)
- [6] Emad Barsoum, John Kender, and Zicheng Liu. Hp-gan: Probabilistic 3d human motion prediction via gan. In *Proceedings of the IEEE conference on computer vision and pattern recognition workshops*, pages 1418–1427, 2018. [2](#)
- [7] Yizhak Ben-Shabat, Xin Yu, Fatemeh Saleh, Dylan Campbell, Cristian Rodriguez-Opazo, Hongdong Li, and Stephen Gould. The ikea asm dataset: Understanding people assembling furniture through actions, objects and pose. In *Proceedings of the IEEE/CVF Winter Conference on Applications of Computer Vision*, pages 847–859, 2021. [2](#), [5](#), [7](#), [11](#), [12](#), [13](#)
- [8] Zhe Cao, Hang Gao, Karttikeya Mangalam, Qi-Zhi Cai, Minh Vo, and Jitendra Malik. Long-term human motion prediction with scene context. In *European Conference on Computer Vision*, pages 387–404. Springer, 2020. [3](#)
- [9] Z. Cao, G. Hidalgo Martinez, T. Simon, S. Wei, and Y. A. Sheikh. Openpose: Realtime multi-person 2d pose estimation using part affinity fields. *IEEE Transactions on Pattern Analysis and Machine Intelligence*, 2019. [3](#), [5](#), [11](#)
- [10] Hsu-Kuang Chiu, Ehsan Adeli, Borui Wang, De-An Huang, and Juan Carlos Niebles. Action-agnostic human pose forecasting. In *IEEE Winter Conference on Applications of Computer Vision, WACV 2019, Waikoloa Village, HI, USA, January 7-11, 2019*, pages 1423–1432. IEEE, 2019. [2](#)
- [11] Christian Diller, Thomas Funkhouser, and Angela Dai. Forecasting characteristic 3d poses of human actions. *arXiv preprint arXiv:2011.15079*, 2020. [2](#), [3](#), [6](#)
- [12] Alexey Dosovitskiy, Lucas Beyer, Alexander Kolesnikov, Dirk Weissenborn, Xiaohua Zhai, Thomas Unterthiner, Mostafa Dehghani, Matthias Minderer, Georg Heigold, Sylvain Gelly, et al. An image is worth 16x16 words: Transformers for image recognition at scale. *arXiv preprint arXiv:2010.11929*, 2020. [6](#)
- [13] Dave Epstein, Boyuan Chen, and Carl Vondrick. Learning the predictability of the future. In *Proceedings of the IEEE/CVF conference on computer vision and pattern recognition*, 2021. [3](#)
- [14] Katerina Fragkiadaki, Sergey Levine, Panna Felsen, and Jitendra Malik. Recurrent network models for human dynamics. In *Proceedings of the IEEE international conference on computer vision*, pages 4346–4354, 2015. [1](#)
- [15] Katerina Fragkiadaki, Sergey Levine, Panna Felsen, and Jitendra Malik. Recurrent network models for human dynamics. In *2015 IEEE International Conference on Computer Vision, ICCV 2015, Santiago, Chile, December 7-13, 2015*, pages 4346–4354. IEEE Computer Society, 2015. [2](#)
- [16] Antonino Furnari and Giovanni Maria Farinella. Rolling-unrolling lstms for action anticipation from first-person video. *IEEE transactions on pattern analysis and machine intelligence*, 43(11):4021–4036, 2020. [1](#)
- [17] Rohit Girdhar and Kristen Grauman. Anticipative Video Transformer. In *ICCV*, 2021. [1](#), [3](#), [5](#), [6](#), [11](#)
- [18] Anand Gopalakrishnan, Ankur Mali, Dan Kifer, C. Lee Giles, and Alexander G. Ororbia II. A neural temporal model for human motion prediction. In *IEEE Conference on Computer Vision and Pattern Recognition, CVPR 2019, Long Beach, CA, USA, June 16-20, 2019*, pages 12116–12125. Computer Vision Foundation / IEEE, 2019. [2](#)
- [19] Tengda Han, Weidi Xie, and Andrew Zisserman. Memory-augmented dense predictive coding for video representation learning. In *European conference on computer vision*, pages 312–329. Springer, 2020. [3](#)
- [20] Catalin Ionescu, Dragos Papava, Vlad Olaru, and Cristian Sminchisescu. Human3.6m: Large scale datasets and predictive methods for 3d human sensing in natural environments. *IEEE Trans. Pattern Anal. Mach. Intell.*, 36(7):1325–1339, 2014. [2](#), [5](#), [11](#), [12](#)
- [21] Ashesh Jain, Avi Singh, Hema S Koppula, Shane Soh, and Ashutosh Saxena. Recurrent neural networks for driver activity anticipation via sensory-fusion architecture. In *2016 IEEE International Conference on Robotics and Automation (ICRA)*, pages 3118–3125. IEEE, 2016. [2](#)
- [22] Ashesh Jain, Amir Roshan Zamir, Silvio Savarese, and Ashutosh Saxena. Structural-rnn: Deep learning on spatio-temporal graphs. In *2016 IEEE Conference on Computer Vision and Pattern Recognition, CVPR 2016, Las Vegas, NV, USA, June 27-30, 2016*, pages 5308–5317. IEEE Computer Society, 2016. [2](#)
- [23] Dinesh Jayaraman, Frederik Ebert, Alexei A Efros, and Sergey Levine. Time-agnostic prediction: Predicting predictable video frames. *arXiv preprint arXiv:1808.07784*, 2018. [3](#)

- [24] Kris M Kitani, Brian D Ziebart, James Andrew Bagnell, and Martial Hebert. Activity forecasting. In *European conference on computer vision*, pages 201–214. Springer, 2012. **1**
- [25] Hilde Kuehne, Ali Arslan, and Thomas Serre. The language of actions: Recovering the syntax and semantics of goal-directed human activities. In *Proceedings of the IEEE conference on computer vision and pattern recognition*, pages 780–787, 2014. **1, 2**
- [26] Miao Liu, Siyu Tang, Yin Li, and James M Rehg. Forecasting human-object interaction: joint prediction of motor attention and actions in first person video. In *European Conference on Computer Vision*, pages 704–721. Springer, 2020. **3**
- [27] Matthew Loper, Naureen Mahmood, Javier Romero, Gerard Pons-Moll, and Michael J. Black. SMPL: A skinned multi-person linear model. *ACM Trans. Graphics (Proc. SIGGRAPH Asia)*, 34(6):248:1–248:16, Oct. 2015. **7**
- [28] Naureen Mahmood, Nima Ghorbani, Nikolaus F. Troje, Gerard Pons-Moll, and Michael J. Black. AMASS: Archive of motion capture as surface shapes. In *International Conference on Computer Vision*, pages 5442–5451, Oct. 2019. **2, 5, 11, 12**
- [29] Wei Mao, Miaomiao Liu, and Mathieu Salzmann. History repeats itself: Human motion prediction via motion attention. In *European Conference on Computer Vision*, pages 474–489. Springer, 2020. **1, 2**
- [30] Wei Mao, Miaomiao Liu, and Mathieu Salzmann. Generating smooth pose sequences for diverse human motion prediction. In *Proceedings of the IEEE/CVF International Conference on Computer Vision*, pages 13309–13318, 2021. **2, 5, 6, 7, 8, 11, 13**
- [31] Wei Mao, Miaomiao Liu, Mathieu Salzmann, and Hongdong Li. Learning trajectory dependencies for human motion prediction. In *Proceedings of the IEEE/CVF International Conference on Computer Vision*, pages 9489–9497, 2019. **1, 2**
- [32] Julieta Martinez, Michael J. Black, and Javier Romero. On human motion prediction using recurrent neural networks. In *2017 IEEE Conference on Computer Vision and Pattern Recognition, CVPR 2017, Honolulu, HI, USA, July 21-26, 2017*, pages 4674–4683. IEEE Computer Society, 2017. **2, 6**
- [33] Georgios Pavlakos, Vasileios Choutas, Nima Ghorbani, Timo Bolkart, Ahmed A. A. Osman, Dimitrios Tzionas, and Michael J. Black. Expressive body capture: 3D hands, face, and body from a single image. In *Proceedings IEEE Conf. on Computer Vision and Pattern Recognition (CVPR)*, pages 10975–10985, 2019. **11**
- [34] Karl Pertsch, Oleh Rybkin, Jingyun Yang, Shenghao Zhou, Konstantinos Derpanis, Kostas Daniilidis, Joseph Lim, and Andrew Jaegle. Keyframing the future: Keyframe discovery for visual prediction and planning. In *Learning for Dynamics and Control*, pages 969–979. PMLR, 2020. **3**
- [35] Nicholas Rhinehart and Kris M Kitani. First-person activity forecasting with online inverse reinforcement learning. In *Proceedings of the IEEE International Conference on Computer Vision*, pages 3696–3705, 2017. **1**
- [36] Marcus Rohrbach, Anna Rohrbach, Michaela Regneri, Sikan-dar Amin, Mykhaylo Andriluka, Manfred Pinkal, and Bernt Schiele. Recognizing fine-grained and composite activities using hand-centric features and script data. *International Journal of Computer Vision*, pages 1–28, 2015. **2, 5, 6, 7, 8, 11, 12, 13**
- [37] Wandu Susanto, Marcus Rohrbach, and Bernt Schiele. 3d object detection with multiple kinects. In *European Conference on Computer Vision*, pages 93–102. Springer, 2012. **11**
- [38] Omid Taheri, Nima Ghorbani, Michael J. Black, and Dimitrios Tzionas. Grab: A dataset of whole-body human grasping of objects. In *Computer Vision – ECCV 2020*, volume LNCS 12355, pages 581–600, Cham, Aug. 2020. Springer International Publishing. **2, 5, 11, 12**
- [39] Yongyi Tang, Lin Ma, Wei Liu, and Wei-Shi Zheng. Long-term human motion prediction by modeling motion context and enhancing motion dynamics. In Jérôme Lang, editor, *Proceedings of the Twenty-Seventh International Joint Conference on Artificial Intelligence, IJCAI 2018, July 13-19, 2018, Stockholm, Sweden*, pages 935–941. ijcai.org, 2018. **2**
- [40] Carl Vondrick, Hamed Pirsiavash, and Antonio Torralba. Anticipating visual representations from unlabeled video. In *Proceedings of the IEEE conference on computer vision and pattern recognition*, pages 98–106, 2016. **3**
- [41] Bastian Wandt, Hanno Ackermann, and Bodo Rosenhahn. 3d reconstruction of human motion from monocular image sequences. *IEEE transactions on pattern analysis and machine intelligence*, 38(8):1505–1516, 2016. **4**
- [42] Bastian Wandt and Bodo Rosenhahn. Repnet: Weakly supervised training of an adversarial reprojection network for 3d human pose estimation. In *Proceedings of the IEEE/CVF Conference on Computer Vision and Pattern Recognition*, pages 7782–7791, 2019. **4, 5, 6, 11**
- [43] Borui Wang, Ehsan Adeli, Hsu-Kuang Chiu, De-An Huang, and Juan Carlos Nieves. Imitation learning for human pose prediction. In *2019 IEEE/CVF International Conference on Computer Vision, ICCV 2019, Seoul, Korea (South), October 27 - November 2, 2019*, pages 7123–7132. IEEE, 2019. **2**
- [44] Yu Wu, Linchao Zhu, Xiaohan Wang, Yi Yang, and Fei Wu. Learning to anticipate egocentric actions by imagination. *IEEE Transactions on Image Processing*, 30:1143–1152, 2020. **2**
- [45] Xinchun Yan, Akash Rastogi, Ruben Villegas, Kalyan Sunkavalli, Eli Shechtman, Sunil Hadap, Ersin Yumer, and Honglak Lee. Mt-vae: Learning motion transformations to generate multimodal human dynamics. In *Proceedings of the European Conference on Computer Vision (ECCV)*, pages 265–281, 2018. **2**
- [46] Ye Yuan and Kris Kitani. Dlow: Diversifying latent flows for diverse human motion prediction. In *European Conference on Computer Vision*, pages 346–364. Springer, 2020. **1, 2, 5, 6, 7, 8, 11, 13**
- [47] Yanjun Zhu, David Doermann, Yanxia Zhang, Qiong Liu, and Andreas Girsensohn. What and how? jointly forecasting human action and pose. In *2020 25th International Conference on Pattern Recognition (ICPR)*, pages 771–778. IEEE, 2021. **3**

Appendix

We show in this appendix additional quantitative and qualitative results (Sec. A and Sec. B), discuss our baseline evaluation protocol (Sec. C), detail the architecture used in our approach (Sec. D), and provide additional details regarding the data (Sec. E).

A. Additional Qualitative Results

Fig. 6 shows additional qualitative results of our method, on both MPII Cooking 2 [36] (left column) and IKEA-ASM [7] (right column).

B. Additional Quantitative Results

Analogous to Tab. 2 in the main paper, Tab. 4 shows an ablation on pose timings and compares our approach of using characteristic poses to poses taken at regular time intervals (“uncoupled”) as well as in the middle or at a random time of an action, on IKEA-ASM [7] data.

C. Baseline Evaluation

We evaluate the performance of our baselines using the same input data that is available to our method. Pose forecasting baselines DLow [46] and GSPS [30] are trained and evaluated on sequences of our manually annotated characteristic poses. Since there is no ground-truth 3D pose data available, we first use RepNet [42], a state-of-the-art 3D pose estimation method, to retrieve 3D skeletons from our 2D characteristic poses. We train this method from scratch using the same database of valid 3D poses that is available to our method.

We train action baseline AVT [17] using sequences of our characteristic pose frames together with the corresponding action labels as input. We use the default parameters used by the original authors for their ablation on third-person dataset 50Salads/Breakfast, inputting our RGB frames instead. For a fair comparison, we also supply the action and object history for each step by encoding both label sequences with a small encoder (a single linear layer) each and fuse these features with the image features generated by the AVT encoder.

We then train two variants of AVT: One with the raw RGB frames, action history, and object history as input (“AVT RGB” in the main results figure), and one with additional 2D skeleton input from the skeletons that we extract with OpenPose [9] (“AVT RGB+Skeleton”).

D. Architecture Details

Fig. 7 shows our architecture in detail with input and output dimensions for linear layers, and the slope for leaky ReLU layers.

E. Data

E.1. Camera Parameters

While intrinsic camera parameters are often available in captured image data, the camera parameters for captured video were not available from the MPII Cooking 2 [36] dataset to use for pose projection. We thus optimized for intrinsic camera parameters from the video sequence data in correspondence with the 3D scene reconstruction of the empty kitchen environment, as given by [37].

E.2. Pose Joint Layout

We use the 9 upper-body joints of the native OpenPose [9] joint layout for skeletons in 2D, and adapt skeletons in our 3D database to use the same format. Tab. 5 shows the correspondence between our joint layout, OpenPose [9], Human3.6m [20], and SMPL-X [33]. 3D datasets AMASS [28] and GRAB [38] provide human bodies in SMPL-X format; we first extract their skeleton joints using their publicly available code and then convert it into our layout using the correspondences in Tab. 5.

E.3. MPII Cooking 2 Details

We use action labels as annotated in the 2D cooking action dataset MPII Cooking 2 [36]. These annotations provide action labels (87 classes) for frame ranges in each sequence as well as the involved objects (187 classes). We first cluster similar actions together, yielding a total of 37 action clusters, which we then use as action classes in our experiments.

In addition, since our goal is to forecast upper-body actions with objects in the foreground, we remove instances of poses and corresponding actions that occur in the background - e.g., when taking out objects from the cupboard, or from the fridge.

In total, there are 272 cooking action sequences; we create a random train/val/test split along sequences with a ratio of 70% / 15% / 15%, yielding 190, 40, 40 sequences for each set.

E.4. IKEA-ASM Details

We use action labels as annotated in the IKEA furniture assembly dataset IKEA-ASM [7]. These annotations provide action labels (31 classes) for frame ranges in each sequence; we use them without explicit object information since each action already encodes its associated object.

In total, there are 370 furniture assembly action sequences; we create a random train/val/test split along sequences with a ratio of 70% / 15% / 15%, yielding 227, 48, 48 sequences for each set.

	2D	3D	Action Accuracy	
Poses	MPJPE [px] ↓	Quality ↑	top-1 ↑	top-5 ↑
Uncoupled	64	0.30	28%	56%
Middle	47	0.35	28%	59%
Random	49	0.24	28%	62%
Characteristic	41	0.35	29%	62%

Table 4. Ablation on pose forecasting, on the IKEA-ASM [7] dataset. We consider predicting poses following state-of-the-art pose forecasting in a decoupled fashion from actions (uncoupled), as well as poses coupled to actions in various fashions: middle (the middle pose of an action range), random (a random pose of the action), and our characteristic pose prediction, which benefits action prediction the most.

Ours		OpenPose		Human3.6m		SMPL-X	
Idx	Name	Idx	Name	Idx	Name	Idx	Name
0	head	0	nose	15	head	15	head
1	neck	1	neck	13	thorax	12	neck
2	right shoulder	2	right shoulder	25	right shoulder	17	right shoulder
3	right elbow	3	right elbow	26	right elbow	19	right elbow
4	right hand	4	right hand	27	right wrist	42	right index 3
5	left shoulder	5	left shoulder	17	left shoulder	16	left shoulder
6	left elbow	6	left elbow	18	left elbow	18	left elbow
7	left hand	7	left wrist	19	left wrist	27	left index 3
8	hip	8	mid-hip	0	hip	0	pelvis

Table 5. Joint layout used in our experiments, for both 2D and 3D skeletons.

E.5. Dataset Contents and Licenses

New Assets. We modify existing datasets for our approach, without creating any assets from scratch. The code and necessary steps for recreating the data will be made public; the license terms of the used datasets prohibit us from directly providing our modified dataset.

Personally identifiable information or offensive content

The datasets used contain footage of humans in action. The original authors of each dataset made sure not to include content that could be used to personally identify the actors involved. There is no offensive content contained in any of the datasets we use or in the modified version created for our approach.

GRAB [38]. The license can be found [here](#). It grants permission to use the dataset for non-commercial scientific research only and prohibits distribution. Consent for using the dataset was given by the original authors, as each user is required to sign up and agree to the license terms prior to downloading any data. All subjects depicted gave written consent allowing their recordings to be used under the terms of this dataset.

AMASS [28]. The license can be found [here](#). It grants permission to use the dataset for non-commercial scientific

research only and prohibits distribution. Consent for using the dataset was given by the original authors, as each user is required to sign up and agree to the license terms prior to downloading any data. All subjects depicted gave consent allowing their recordings to be used under the terms of this dataset.

Human3.6m [20]. The license can be found [here](#). It grants permission to use the dataset for academic use only and prohibits distribution. Consent for using the dataset was given by the original authors, as each user is required to sign up and agree to the license terms prior to downloading any data. All subjects depicted are professional actors who gave consent allowing their recordings to be used under the terms of this dataset.

MPII Cooking 2 [36]. The license can be found [here](#). It grants permission to use the dataset for academic use only and prohibits redistribution. Consent for using the dataset was given implicitly by the original authors, as the data is freely accessible from their website, under their license terms. All subjects depicted are paid students who gave consent allowing their recordings to be used under the terms of this dataset.



Figure 6. Additional qualitative comparison between DLow [46], GSPS [30], and our method on two sequences (left on MPII Cooking 2 [36], right on IKEA-ASM [7]). For each method, we show a the 3D predicted pose projected into the 2D target view, without background for a pose only version (first row) as well as with background for context (second row).

IKEA-ASM [7]. The license can be found [here](#). It is licensed under the terms of the Creative Commons Attribution-NonCommercial 4.0 International License which means it may be used for research and educational purposes as long as appropriate credit is given. All subjects depicted gave consent allowing their recordings to be used under the terms of this dataset.

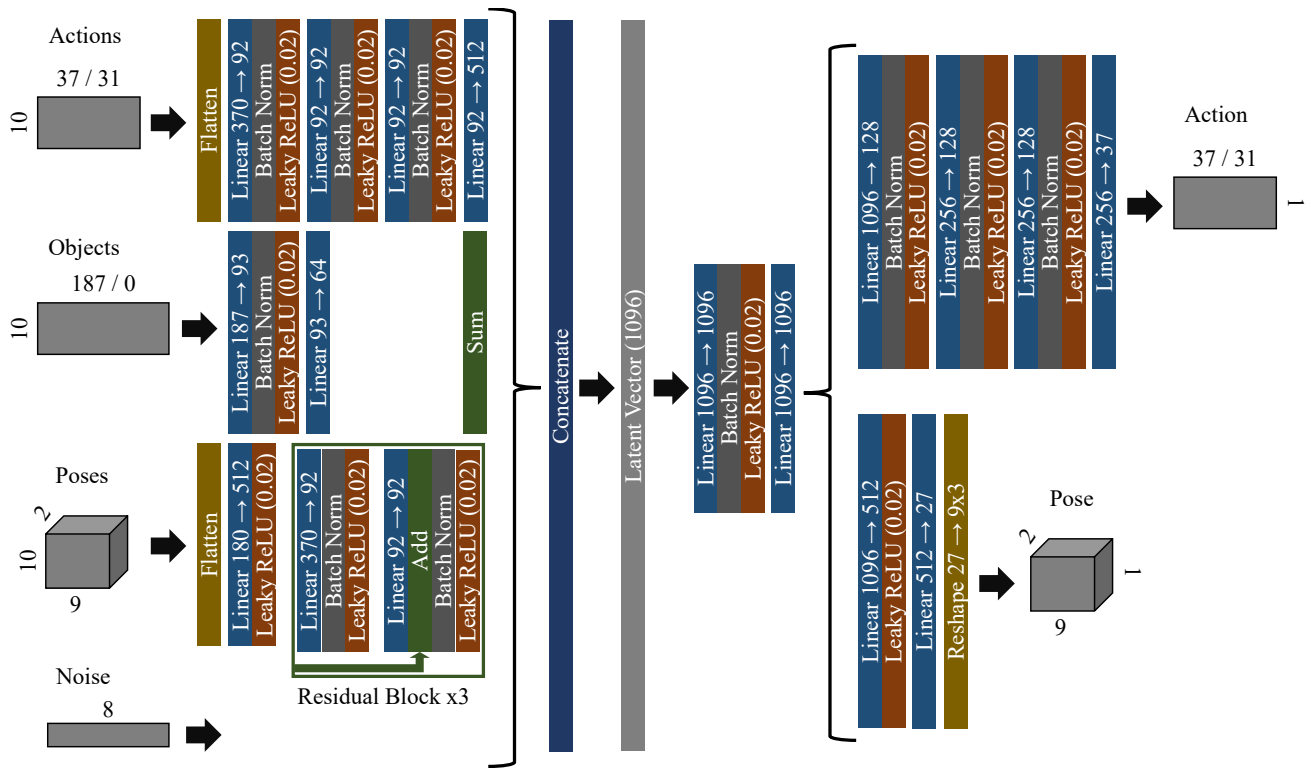


Figure 7. Network architecture specification.